

School of Meteorology, University of Oklahoma, Norman, USA

Dispersion of passive tracer in the atmospheric convective boundary layer with wind shears: a review of laboratory and numerical model studies

E. Fedorovich

With 9 Figures

Received July 5, 2003; revised August 9, 2003; accepted September 21, 2003

Published online: June 2, 2004 © Springer-Verlag 2004

Summary

Paper reviews recent laboratory and numerical model studies of passive gaseous tracer dispersion in the atmospheric convective boundary layer (CBL) with surface and elevated wind shears. Atmospheric measurement data used for validation of these two model techniques are briefly discussed as well. A historical overview is given of laboratory studies of dispersion in the atmospheric CBL. Model studies of tracer dispersion in two CBL types, the (i) non-steady, horizontally homogeneous CBL and (ii) quasi-stationary, horizontally heterogeneous CBL, are reviewed. The discussion is focused on the dispersion of non-buoyant plume emitted from a point source located at different elevations within the CBL. Approaches towards CBL modeling employed in different laboratory facilities (water tanks and wind tunnels) are described. The reviewed numerical techniques include Large Eddy Simulation (LES) and Lagrangian modeling. Numerical data on dispersion in the sheared CBL is analyzed in conjunction with experimental results from wind-tunnel CBLs.

1. Introduction

Convective boundary layers (CBLs) driven by buoyancy forcings from the bottom or/and from the top and capped by temperature (density) inversions are commonly observed in the lower portion of earth's atmosphere (Holtslag and Duynkerke, 1998). During fair-weather daytime conditions, in the absence of clouds (which is the

case of clear CBL, see op. cit.), the buoyancy forcing in the boundary layer is primarily represented by convective heat transfer from a warm underlying surface. This feature is an apparent reason for calling the considered boundary-layer type "convective" in the meteorological and other geophysical applications of fluid mechanics. The term "convective" also emphasizes the fact that buoyant convection is the main mechanism of turbulence production in the boundary layer, whilst the contribution of wind shear to the generation of turbulence is of secondary importance.

The surface buoyancy forcing generates up-and downward motions that effectively mix momentum and scalar fields inside the CBL. The fast rising updrafts (convective thermals) typically occupy a smaller percentage of the CBL horizontal cross-sectional area than the broader, but more slowly descending convective motions, or downdrafts (Lenschow, 1998). Due to active mixing, the wind velocity, potential temperature (buoyancy), and concentrations of atmospheric constituents in the main portion of the CBL (often referred to as convectively mixed layer) do not change considerably with height when averaged over horizontal planes or over time. A typical CBL can be subdivided into three

separate layers: the surface layer, in which the meteorological variables change fairly rapidly with height; the mixed layer, where mean vertical gradients of these variables are close to zero; and the entrainment zone (also referred to as the inversion layer or interfacial layer), where again the large gradients in meteorological fields are observed. Across the entrainment zone, the free-atmosphere air, which is more buoyant than the CBL air, is entrained into the convectively mixed layer as the CBL grows. Such convective entrainment is maintained by the penetration of the thermals into the stably stratified atmosphere above the CBL and subsequent folding of more buoyant air from aloft into the CBL as these overshooting thermals sink back into the mixed layer.

Flow-field and concentration patterns in the atmospheric CBL are strongly variable both in time and in space. However, in the meteorological boundary-layer studies, two CBL types different with respect to their spatial-temporal evolution are usually considered. The first CBL type (we will call it the non-steady CBL) is (or assumed to be) statistically quasi-homogeneous over a horizontal plane. In this case, the CBL evolution is regarded as a non-stationary process. Most numerical and laboratory CBL studies reported in the literature have been carried out within the assumption of horizontal homogeneity of the layer. Available field measurement data on the turbulent flow structure and dispersion of passive constituents in the CBL usually also refer to this CBL type. Another commonly studied case of the atmospheric CBL is the horizontally evolving CBL, which grows in a neutrally or stably stratified air mass that is advected over a heated underlying surface. This type of the CBL (we will call it the heterogeneous CBL) is a traditional subject of wind-tunnel model studies. Based on the Taylor hypothesis (Willis and Deardorff, 1976b), it is generally possible to relate temporal and spatial scales of dispersive turbulent motions in the non-steady and heterogeneous CBLs (Fedorovich et al, 1996).

The turbulence structure and characteristics of dispersion in the atmospheric CBL have been rather thoroughly investigated for the case of CBL without wind shears (hereafter referred to as the case of shear-free CBL). Just a few studies have been devoted to the investigation of effects produced by additional non-convective (or non-

buoyant) forcings that contribute to the CBL turbulence regime in conjunction with the dominant buoyant driving mechanism. Examples of such forcings are wind shears and surface roughness. In the developed CBL, the momentum field inside the layer is well mixed by convective motions and, as shown in Garratt et al (1982), the flow regions with strong mean wind gradients (shears) are usually located at the surface (surface shear) and at the level of inversion (elevated shear).

The present paper reviews recent laboratory and numerical model studies of passive tracer dispersion in the atmospheric CBL with wind shears. The atmospheric measurement data available for validation of these model approaches will be briefly presented as well, although I know of no major CBL dispersion field experiments conducted recently. A historical overview will be given of laboratory models of dispersion in the atmospheric CBL. Model studies of tracer dispersion in the both aforementioned CBL types (non-steady and heterogeneous) will be reviewed. The discussion will be focused on the dispersion of non-buoyant plume of tracer emitted from a point source located at different elevations within the CBL.

2. Laboratory models of dispersion in the CBL

The pioneering laboratory studies of gaseous plume dispersion in the atmospheric CBL have been performed in the 1970s and 1980s by Willis and Deardorff (1976a; 1978; 1981; 1983; 1987), and Deardorff and Willis (1982; 1984). These experiments, conducted in convection water tank heated from the bottom, demonstrated the complexity of tracer concentration patterns in the CBL and their sensitivity to the turbulence regime of the CBL.

In order to imitate a mean wind in the CBL, a model stack in the quoted laboratory experiments was towed along the bottom of convection water tank. Apparently, this technique only partially accounts for the effect of wind on the tracer dispersion. The mean advection of tracer is adequately reproduced in this case, while turbulent diffusive motions generated due to bottom friction and vertical shears are not taken into account. In an attempt to overcome this limitation of water-tank

modeling techniques, an idea of composite water tank was realized in the recent laboratory study of Park et al (2001). Such composite water tank system includes a conventional water tank, similar to the one used in the experiments of Willis and Deardorff, and a moving grid plate for mechanical generation of turbulence near the bottom of the tank, which is intended to simulate the shear-produced turbulence. With mechanically generated turbulence, the authors of op. cit. managed to achieve rather close agreement between their laboratory and CONDORS field experiment (Briggs, 1993) data on the vertical dispersion variation as function of distance from the source.

As a tool for dimensionless analysis and interpretation of plume dispersion pattern in the laboratory CBL, Willis and Deardorff applied the Deardorff (1970b) convective (mixed-layer) scaling, further discussed in Deardorff (1985), which since that time has served as standard framework for inter-comparison of CBL dispersion data from different sources. This scaling has been originally proposed to normalize mean-flow parameters and turbulence statistics in the numerically simulated pure case of shear-free CBL. The scaling concept is based on three governing scales for length: z_i , velocity: w_* , and temperature (which should be considered as virtual potential temperature in the case of clear atmospheric CBL): T_* . The length scale z_i (interpreted as the CBL depth) is taken as the elevation the level of the most negative heat flux of entrainment within the interfacial layer, the velocity scale is related to z_i and to the surface kinematic heat flux Q_s as $w_* = (\beta Q_s z_i)^{1/3}$, where $\beta = g/T_0$ is the buoyancy parameter (g is the acceleration due to the gravity, T_0 is the reference temperature), and the temperature scale is defined through the ratio of Q_s to w_* : $T_* = Q_s/w_*$. For the purpose of normalization of concentration patterns in the CBL with mean wind, the above original scaling has to be complemented with the horizontal length scale $L_h = (z_i \cdot U)/w_*$, and the concentration scale $c_* = E_s/(z_i^2 \cdot U)$, where U is the mean wind velocity and E_s is the tracer source strength in units of volume per unit time (Deardorff, 1985). Two other dimensionless parameters (numbers) based on the Deardorff (1970b) convective scales are commonly employed to characterize turbulence regime in the CBL developing on the background of stable

stratification (see, e.g., Deardorff et al, 1980; Zilitinkevich, 1991; Fedorovich and Mironov, 1994): the Richardson number Ri_{AT} related to the temperature increment ΔT across the interfacial layer: $Ri_{AT} = \beta w_*^{-2} z_i \Delta T$, and the Richardson number based on the buoyancy frequency N in the turbulence-free zone above the CBL: $Ri_N = N^2 z_i^2 w_*^{-2}$.

Willis and Deardorff (1978) found in their water tank experiments that the source location is an important factor of the concentration distribution in the CBL. They have shown, see also Lamb (1982), that the average centerline of the plume released from an elevated source in the CBL descends quickly downwind of the source. In contrast, the plume released near the surface rises fast inside the CBL. These observations, which are not consistent with predictions of the Gaussian plume model, manifest the specific character of dispersion in the CBL associated with the skewed (narrow, fast updrafts versus broad, slow downdrafts) vertical velocity field.

The water-tank experiments of Willis and Deardorff significantly advanced our understanding of dispersion in the CBL, but were limited by measurement and data processing techniques. The original tank, which was used in those experiments, no longer exists: it was acquired by the Fluid Modeling Facility of EPA and profoundly modified over the years to such an extent that nothing remains of the original except for dimensions, as described in Snyder et al (2002). The new tank is equipped with laser-induced-fluorescence and video-imaging systems for making non-intrusive measurements of tracer concentrations, as well as with computerized control system that enables all operation and measurement functions to be specified and controlled though a single procedure. The main idea behind the tank renovation has been the establishing of a laboratory tool to study the dispersion of highly buoyant plumes in the CBL (Weil et al, 2002), which was not sufficiently studied previously in the laboratory. However, a series of experiments in the new tank have also been conducted with non-buoyant plumes. For the mean concentration fields and for some other plume dispersion characteristics (for instance, the concentration intermittency and the lateral dispersion variation), the new data displayed trends similar to those found earlier by Willis

and Deardorff. A good agreement has been also found with field data from Hanna and Paine (1989) on ground-level concentrations and with analytical predictions for the lateral dispersion in the CBL. Some discrepancies between the new results and Willis and Deardorff data have been attributed by Weil et al (2002) to the insufficient sampling in the early water tank experiments (this sampling problem, however, seems to affect more the experiments with buoyant plumes).

Another type of laboratory facility employed for CBL dispersion studies is a saline water tank. An example of such a facility, described in Hibberd and Sawford (1994a, b), has been used for investigation of various CBL dispersion regimes, in particular the plume fumigation into a growing shear-free CBL (Hibberd and Luhar, 1996). The experiments in the saline tank are performed in an upside-down fashion (the source of negative buoyancy is located at the top) as compared to the water tank heated from the bottom. The saline-tank approach towards CBL modeling has its own advantages and disadvantages. The main advantage is the possibility of accurate control of the steadiness of stratification in a tank without caring about heat losses. The developers of the saline-tank CBL model (Hibberd and Sawford, 1994a) claim that at typical laboratory scales, saline convection can satisfy the requirements for modeling buoyant plume dispersion under strongly convective (light wind) conditions better than thermal convection in heated water tanks.

Nevertheless, the discussed water-tank CBL model approaches either omit or treat rather indirectly the effects of wind shears on the turbulence regime and characteristics of dispersion in the atmospheric CBL. With respect to taking these effects into account, the wind-tunnel model approach seems to be the most feasible one. A series of laboratory studies of plume dispersion in a sheared CBL have been conducted in specially designed thermally stratified wind tunnels in different countries of the world, see reviews by Meroney and Melbourne (1992), and Meroney (1998).

First wind-tunnel experiments of this kind have been carried out in the Colorado State University by Poreh and Cermak (1985). They have measured parameters of the three-dimensional plume spread in the horizontally evolving CBL

and found them to be in a fair qualitative agreement with atmospheric observations.

A number of wind tunnel facilities capable of simulating the atmospheric CBL have been constructed during the two past decades in Japan. Recent CBL flow and dispersion experiments conducted in two of these facilities are described in Sada (1996), and Ohya et al (1996; 1998). The tunnel used by the latter research team is probably the most technologically advanced facility among existing thermally stratified tunnels all over the world. Sada (1996) studied a tracer diffusion in a CBL with weak wind shear using the thermally stratified wind tunnel of Komae Research Laboratory. He found the Deardorff (1970b) convective scaling to be applicable to the flow and diffusion patterns in the simulated CBL. The capping temperature inversion in the conducted wind-tunnel experiments was rather weak. That was a reason for substantial vertical spread of the plume in the upper portion of the wind-tunnel CBL. In the op. cit., the experimentally obtained parameters of dispersion were not analyzed in conjunction with properties of turbulence in the simulated CBL, and effects of flow shear on the tracer dispersion in the CBL were not particularly investigated.

The first real opportunity to study in laboratory the effects of wind shears on dispersion in the CBL was presented in the beginning of the 1990s, when a thermally stratified wind tunnel was completed at the University of Karlsruhe (UniKa), Germany, by M. Rau and his colleagues (Poreh et al, 1991; Rau et al, 1991; Rau and Plate, 1995). Characteristics of turbulent flow in the quasi-stationary, horizontally evolving, sheared atmospheric CBL simulated in the UniKa wind tunnel have been comprehensively studied by Fedorovich et al (1996), Kaiser and Fedorovich (1998), and Fedorovich and Kaiser (1998). These wind-tunnel experiments have shown that wind shears can essentially modify the turbulence dynamics in the CBL and parameters of turbulent exchange (entrainment) across the capping inversion. Later on, the wind-tunnel studies at UniKa have been complemented by numerical Large Eddy Simulation (LES) of the CBL flow case reproduced in the tunnel (Fedorovich et al, 2001a, b; Fedorovich and Thäter, 2001). This combination of numerical and laboratory approaches allowed a detailed

quantification of mean flow characteristics and turbulence statistics in the convectively driven flow modified by surface and elevated wind shears. Parallel to the basic CBL flow studies, the UniKa wind-tunnel group conducted a series of tracer dispersion experiments in the CBL with wind shears (Thäter et al, 2001; Fedorovich and Thäter, 2001).

In order to account for the contribution of wind shears to the turbulence regime of the CBL, one has to complement the list of CBL flow parameters by new quantities that are representative of shear effects. Dynamic effect of the surface shear is commonly characterized by the friction velocity $u_* = \tau_s^{1/2}$, where τ_s is the near-surface value of $\tau = \sqrt{(\overline{w'u'})^2 + (\overline{w'v'})^2}$, the turbulent shear stress magnitude normalized by density. There is no commonly accepted parameter to characterize the elevated wind shear. A reasonable candidate for this function could be the entrainment shear velocity $s_* = (\Delta u^2 + \Delta v^2)(dz_i/dt)$ discussed in Fedorovich (1995) and applied for parameterization of the shear effects on the CBL growth in Pino et al (2003). In the above formula, elevated wind shear is expressed in terms of zero-order jumps of horizontal wind velocity components u and v across the entrainment zone. If we now relate velocity scales u_* and s_* to the governing velocity scale w_* representing the buoyancy forcing, we will come up with two dimensionless combinations u_*/w_* and s_*/w_* characterizing, respectively, the contributions of surface and elevated shears, to the turbulence dynamics in the CBL. The first of these combinations can be expressed in terms of the Monin-Obukhov length $L = -u_*^3/(\beta k Q_s)$ and the CBL convective length scale z_i ratio: $u_*/w_* = -(kL/z_i)^{1/3}$, as described, e.g. in Fedorovich et al (1996). Following Holtslag and Nieuwstadt (1986), the shear contribution to the turbulence production in the CBL (in the absence of elevated shear) can be neglected if $-L/z_i < 0.1$, which gives $u_*/w_* = 0.34$ as a conventional boundary value to distinguish between the regimes of shear and shear-free convection.

3. Modification of CBL flow by wind shears

The effect of surface shear on the CBL flow structure has been extensively investigated dur-

ing the last two decades by means of numerical Large Eddy Simulation (LES). The LES technique was for the first time employed in the atmospheric CBL studies by Deardorff (1970a). Since that time, this technique has been considerably developed and applied to different types of atmospheric and industrial boundary-layer flows, see review papers by Mason (1994), Lesieur and Métais (1996), Piomelli and Chasnov (1996). The LES approach distinguishes between large-scale energy-carrying anisotropic motions (large eddies), which are resolved explicitly on the numerical grid employed, and smaller subgrid motions, which are assumed to be homogeneous and isotropic, and therefore can be parameterized with a universal turbulence closure scheme. In order to separate the effects of large eddies and small-scale motions in the computational procedure, the initial flow-governing equations describing all scales of motions are filtered, and the terms responsible for the effects of subgrid motions (subgrid-scale stresses and fluxes) appear in the filtered LES equations as additional source terms. It is clear from the nature of LES that the success of its application for the reproduction of high Reynolds number turbulent flows essentially depends on the complexity of small-scale motions to be parameterized, and the proportion of energy contents between the resolved and subgrid scales of motion.

One of the first numerical studies aimed at the evaluation of shear effects in the CBL has been conducted by Sykes and Henn (1989). Although the CBL case reproduced in this study was not exactly relevant to the atmospheric CBL, the results obtained have nevertheless provided a quantitative estimate of the ability of an externally applied shear to organize the convective eddies into two-dimensional rolls. The combined effects of wind shear and buoyancy forces in the atmospheric CBL have been investigated in the LES study by Moeng and Sullivan (1994). They observed a similar re-organization of the turbulence structure when the shear-free convection regime in the boundary layer has been replaced by sheared convection. As the contribution of wind shear grew, elongated high-low-speed streaks were formed in the near-surface region of the simulated boundary-layer flow replacing the irregular polygonal structure characteristic of the shear-free convective flow. Mason (1992)

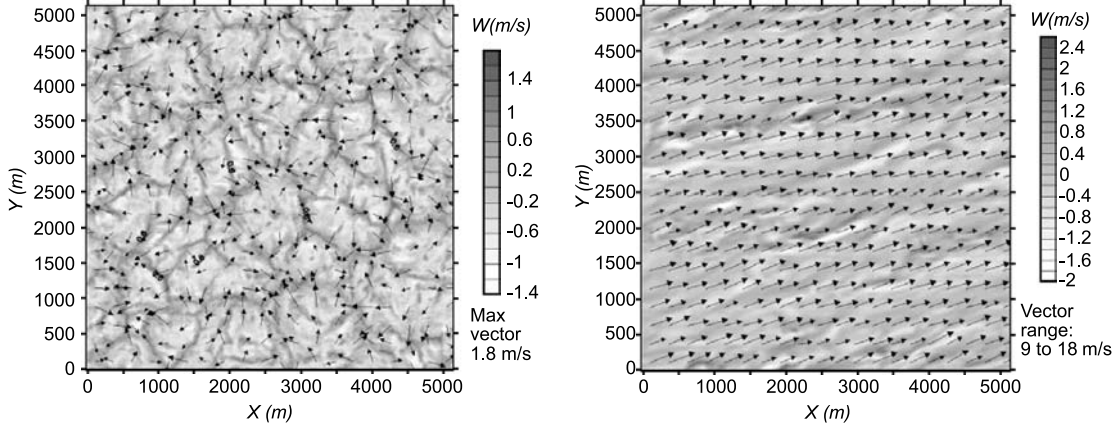


Fig. 1. Simulated structure of near-surface u and v (arrows), and w (shaded contours) fields in the case of shear-free CBL (left plot) and in the CBL with strong (20 m/s) height-constant geostrophic wind (right plot); from Conzemius and Fedorovich (2003)

applied LES to study dispersion of a passive scalar in a CBL with wind shear. He found that a relative increase of shear with respect to buoyancy led to an increase of short-time dispersion rates. In contrast, the vertical dispersion at greater time was reduced and took on the character of a simple diffusive process. Mason linked this marked change in vertical dispersion to the effect of a reduced length scale in shear-driven turbulence compared with convective turbulence. All aforementioned LES studies have generally confirmed 0.34 to be a critical value of the shear/buoyancy production ratio separating shear-free and sheared convection regimes in the CBL.

In a comprehensive LES study of the three-dimensional structure of buoyancy- and shear-induced turbulence in the atmospheric boundary layer, Khanna and Brasseur (1998) spanned a vast range of stability conditions starting from a nearly shear-free CBL ($-L/z_i = 0.0014$, $u_*/w_* = 0.0047$) to an almost purely shear-driven boundary layer ($-L/z_i = 2.3$, $u_*/w_* = 7.7$). Besides the general support of earlier findings by Moeng and Sullivan (1994) concerning the shear-induced alteration of the CBL coherent structure, this study provided further insights into the individual properties of convective thermals and rolls. Based on the comparison of visualizations of structures with turbulence spectra in the buoyancy-driven flow, Khanna and Brasseur concluded that the shear-dominated near-surface

structure of the unstable surface layer influences directly the global structure of the moderately convective boundary layer.

In Fig. 1, near-surface flow velocity fields in the shear-free and strongly sheared CBLs from the LES study of Conzemius and Fedorovich (2003) are demonstrated. The aforementioned differences between the CBL flow structures (cells in the shear-free CBL versus rolls in the sheared CBL) in these two cases are clearly seen in the plots.

Modification of the CBL turbulence regime by surface shear has been investigated experimentally by Fedorovich et al (1996), and Kaiser and Fedorovich (1998) in the UniKa wind-tunnel model of a horizontally evolving CBL. In these experiments, surface shear was found to be an essential contributor to the turbulence production. Values of the surface shear-to-buoyancy production ratio u_*/w_* of 0.3 and larger resulted in a noticeable increase in the variance of velocity fluctuations in the lower portion of the layer compared with their counterparts in the shear-free CBL. Weak roll-like semi-organized motions were identified in the pattern of mean velocity measured in planes perpendicular to the mean flow direction. In the bulk of the CBL, buoyancy was found to be the dominant factor of turbulence production at smaller wave numbers, while the shear contribution was apparently increasing towards large wave numbers. The surface shear forcing in the simulated CBL

was suggested to be a reason for the elongation and flatness of the production ranges in the measured velocity spectra.

Compared to the effect of shear at the surface, the influence of wind shear across the capping inversion (elevated shear) on CBL turbulence is much less studied. Such elevated shears are typically observed in the atmospheric CBL under baroclinic conditions (Stull, 1988). The velocity increments across the inversion layer in this case can be of either sign depending on the geostrophic wind change with height in terms of the so-called thermal wind (Fedorovich, 1995). According to the zero-order jump CBL model, the contribution of elevated shear to the production of turbulent kinetic energy in the growing CBL ($dz_i/dt > 0$) is essentially positive.

At the same time, wind-tunnel experiments of Fedorovich and Kaiser (1998) have provided an indication that turbulence enhancement in the upper portion of the horizontally evolving CBL with elevated shears may be accompanied by the decrease of the CBL growth rate. Due to technical restrictions, the aforementioned experiments could only be conducted with positive shear across the inversion layer, when the flow in the outer turbulence-free region had larger mean momentum than the turbulent flow in the bulk of the CBL. In the complementary LES study, Fedorovich et al (2001b) tried to associate this damping effect of elevated shear on the CBL growth with the so-called shear sheltering of turbulence previously considered by Csanady (1978), Jacobs and Durbin (1998), Hunt and Durbin (1999), and in connection with cross-wind effects in the inversion layer by Hunt (1998).

In their LES output, Fedorovich et al have discovered what they called the directional effect of elevated shear on the growth of the horizontally evolving CBL. In the case of positive wind shear across the inversion layer (the flow above the inversion possesses a larger momentum than mean motion in the mixed layer), the CBL growth has been found impeded compared to the case of CBL with the shear-free inversion, just in accordance with the experimental findings of Fedorovich and Kaiser (1998). On the other hand, the LES experiments have revealed the activation of boundary-layer growth in the case of elevated negative shear when the mean flow above the inversion possesses a smaller horizon-

tal momentum than mean motion in the mixed layer. In this way, the effect of negative elevated shear on the CBL growth turned out to be opposite to that of the positive shear.

A subsequent numerical study of Fedorovich and Thäter (2001) suggested that Fedorovich et al (2001b) had correctly identified the modifications of turbulence structure in the CBL with sheared capping inversion but overlooked the main effect of elevated wind shear on the flow dynamics in the horizontally evolving CBL. This main effect was associated with local organized vertical motions at the CBL top due to acceleration or deceleration of the CBL flow caused by momentum transport across the sheared capping inversion. The acceleration of the CBL flow (the increase of the u component of mean motion with x below the capping inversion) took place in the positive-shear case. Due to the fluid continuity it produced negative (descending) mean vertical motion at the level of inversion. The opposite happened in the negative-shear case, when the upward transport of momentum across the inversion caused the deceleration of mean flow within the CBL. This deceleration led to positive (ascending) organized vertical motion pushing the capping inversion upwards. In the positive-shear case, the generated mean vertical motion opposed the entrainment at the CBL top and thus slowed down the CBL growth, whilst in the case of negative shear, the organized upward motion supported the CBL growth in addition to the entrainment mechanism.

The discussed effect of elevated shear on the CBL evolution is essentially a feature of the horizontally evolving CBL. Indeed, under the conditions of horizontal (quasi-) homogeneity in the non-steady CBL, there is no internal source of mean vertical motion at the CBL top that can adversely modify the sign of the CBL growth. Recently, there were several numerical (LES) studies reported that specifically addressed the role of elevated shear in the convective entrainment and the CBL development. These studies arrived at rather mixed conclusions. On one hand, numerical experiments of Pino et al (2003) provided an indication of unconditional enhancement of the entrainment and CBL growth rate by the combined effect of surface and elevated shears. On the other hand, numerical results of Conzemius and Fedorovich (2002) gave no clear

indication of wind shear contribution to the CBL growth dynamics. A systematic additional investigation of considered effects by Conzemius and Fedorovich (2003), who simulated nine CBL flow cases with variable shear and buoyancy forcings, has shown that strong wind shear can significantly enhance the CBL growth rate when heat flux at the lower surface is weak and the stratification of the atmosphere above the CBL is moderate or weak. If the surface heat flux and the outer-atmosphere stratification are both strong, the effect of shear on the CBL growth, in a relative sense, becomes negligible. Nevertheless, shear in this case still exerts a strong influence over the turbulence structure within the CBL. The conducted numerical experiments did not provide any direct support for the Hunt and Durbin (1999) theory of turbulence shear sheltering in the case of a CBL-type flow.

Main results recently obtained with laboratory and numerical models regarding the wind shear influence on turbulent flow in the atmospheric CBL may be summarized as follows.

- (1) Variances of horizontal velocity components in the lower (up to $z/z_i = 0.5$) portion of the CBL are noticeably enhanced in the presence of surface shear.
- (2) Surface wind shear does not significantly affect the temperature variance and vertical heat flux in the main portion of the CBL.
- (3) Longitudinal roll-like structures formed in the sheared CBL additionally contribute to the variance of the across-wind velocity component.
- (4) Elevated wind shear generates larger variances of longitudinal velocity component in the entrainment zone (interfacial layer) at the CBL top.
- (5) Wind shears lead to broader production ranges in the velocity fluctuation spectra extended towards larger wave-number values.

- (6) In the horizontally heterogeneous CBL, elevated wind shears of different signs have a directional effect on the entrainment and variation of the CBL depth with distance.

4. Plume dispersion in the horizontally evolving CBL

In this section, the review will be given of recent laboratory and numerical studies of gaseous plume dispersion in the quasi-stationary, horizontally inhomogeneous CBL flow. Laboratory studies of dispersion regimes were conducted in the UniKa thermally stratified wind tunnel in 1996–2001. They were complemented in 2000–2001 by LES of dispersion in the considered CBL flow case.

The UniKa wind tunnel is a facility of the closed-circuit type, with 10-m long, 1.5-m wide and 1.5-m high test section. The return section of the tunnel is subdivided into ten layers, which are individually insulated. Each layer is 15-cm deep and is driven by its own fan and heating system. In this manner, the velocity and temperature profiles can be pre-shaped at the inlet of the test section as shown in Fig. 2. The test section floor can be heated with a preset energy input to produce a constant heat flux through the CBL bottom. The CBL in the tunnel develops through several intermediate regimes that are described in Fedorovich et al (2001a). The stage of quasi-homogeneous, slowly evolving CBL, which is the closest counterpart of the atmospheric CBL, is achieved at $x \approx 5.5$ m.

At this stage, the value of Ri_{AT} is the wind-tunnel CBL model is about 10, which is one order of magnitude smaller than typical Ri_{AT} values in majority of numerical and water-tank CBL models. For most of cases studied in the tunnel, the value of u_* was from 0.03 to

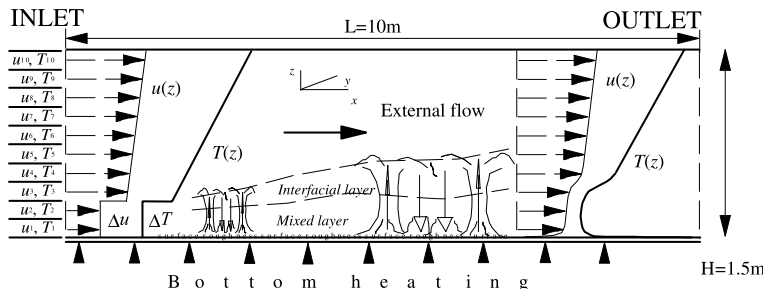


Fig. 2. Sketch of modeling the horizontally evolving, sheared atmospheric CBL in the UniKa thermally stratified wind tunnel

0.08 m/s and w_* – from 0.15 to 0.20 m/s, and thus the u_*/w_* ratios were within the range from 0.2 to 0.5 ($0.02 < -L/z_i < 0.3$), that is around the margin for the surface shear effects (see estimates in Sect. 3). For the diffusion experiments in the tunnel, a non-buoyant tracer has been used. As tracer gas, SF₆ has been employed. The mixture of tracer gas with air was emitted in the central vertical plane of the tunnel at 3.32-m distance from the test-section inlet, close to the downwind edge of established CBL region. Concentration measurements have been made using standard technique based on the electron detector method. The measured concentration values have been averaged over two-minute time periods. For additional information regarding the experimental setup see Fedorovich and Thäter (2002).

In Fig. 3, the longitudinal concentration distribution from a near-ground source in the sheared wind-tunnel CBL is plotted together with its counterpart from the Willis and Deardorff (1978) water-tank model of the shear-free CBL. From the qualitative point of view, the concentration distributions provided by both experimental techniques fairly agree with each other (one should keep in mind that the Taylor hypothesis was employed to enable comparability of the wind-tunnel distribution with the water-tank distribution). In both CBL models, the plume released near the surface rises fast inside the layer, which is a well-known feature of plume dispersion in the CBL (Lamb, 1982). However, a closer inspection of the plots reveals the

smaller horizontal concentration gradients in the lower portion of wind-tunnel CBL. This is apparently a result of enhanced longitudinal transport of tracer by comparatively large horizontal velocity fluctuations associated with surface shear in the wind-tunnel flow.

In Fig. 4, a concentration distribution measured in the wind-tunnel CBL with imposed positive elevated shear (second plot from the top) is compared with its analog for the case of CBL with a shear-free upper interface (the uppermost plot). Demonstrated concentration patterns refer to the central vertical plane of the tunnel. Concentration values in the plots are normalized as $c_* = c \cdot L^2 \cdot U/E_s$, where $L = 1$ m, $U = 1$ m s⁻¹. The presented comparison indicates that in the considered CBL case, the elevated positive shear amplifies the effect of stable stratification in obstructing the plume penetration above the inversion, which leads to a pronounced blocking of the tracer within the CBL. The resulting concentration levels at the same elevations along the wind-tunnel test section are noticeably smaller in the case of sheared inversion than in the CBL capped by a shear-free density interface. As one may also notice, the rise of the maximum concentration line in the case of sheared inversion is delayed in comparison with the reference shear-free case. The enhanced horizontal velocity fluctuations inside the sheared inversion lead to comparatively smooth horizontal distribution of concentration in the upper portion of CBL with elevated shear (second plot from the top in Fig. 4).

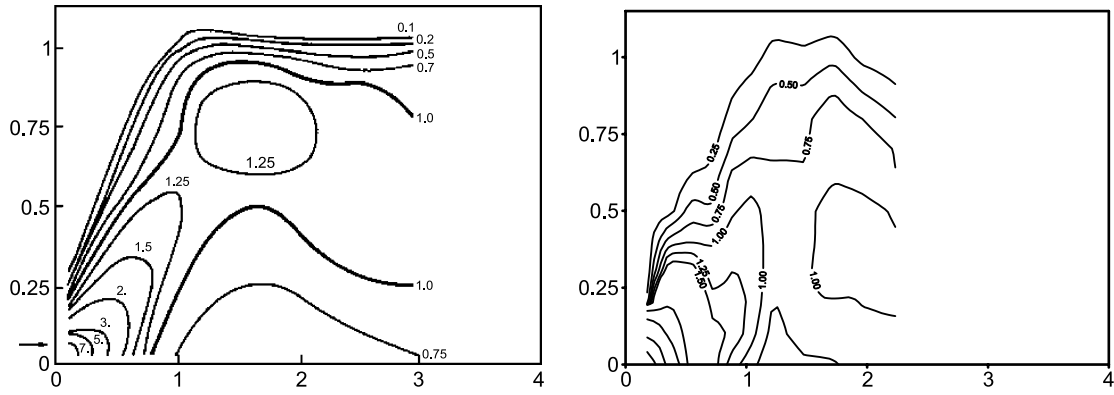


Fig. 3. Dispersion of a non-buoyant plume in the water-tank model of shear-free CBL (Willis and Deardorff, 1978, left plot) and in the UniKa wind tunnel CBL (Fedorovich and Thäter, 2002, right plot). The source elevation is $z/z_i = 0.07$. Height, length, and concentration are normalized by Deardorff (1970b; 1985) convective scales. The origin of the x -ordinate is at the source location

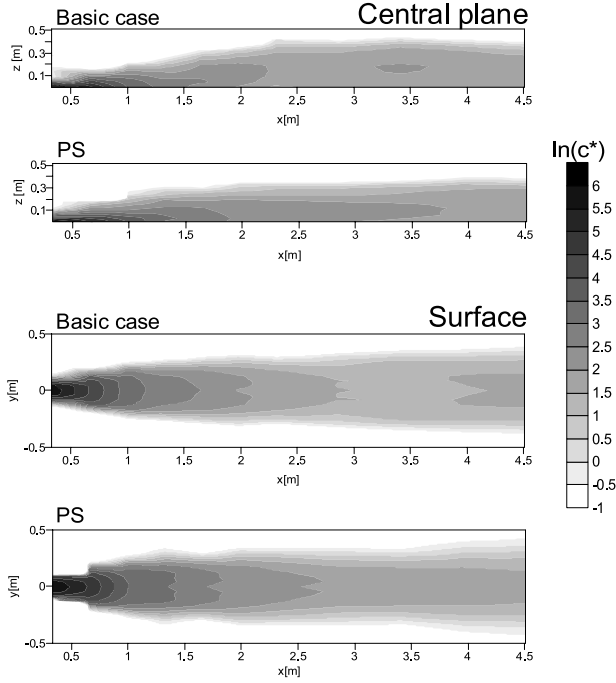


Fig. 4. Longitudinal concentration distributions measured in the CBL with positive elevated wind shear (PS) and in the basic CBL flow case without elevated shear (denoted as Basic case). The source is at the ground level in both cases. The origin of the x -ordinate is at the source location. The capping-inversion and shear-zone elevations at $x=0$ are 0.3 m

In the CBL with positive elevated shear, the ground concentrations are generally higher than in the CBL flow with a shear-free inversion layer (compare two lower plots in Fig. 4). This is a result of accumulation of tracer in the congested and more shallow boundary layer affected by the elevated wind shear.

Further results from the described wind-tunnel experiments, summarized in Fedorovich and Thäter (2002), indicate that the cross-stream concentration distribution in the sheared CBL displays features of plume channeling, which is presumably caused by longitudinal semi-organized roll-like motions in the CBL with shear.

A numerical study of dispersion in the UniKa wind-tunnel CBL was conducted by means of the LES code described Fedorovich et al (2001a) with an added dispersion simulation block (Thäter et al, 2001). The Eulerian method considered in Nieuwstadt (1998) was employed for incorporation of the tracer transport in the LES framework, and the balance equation for the

tracer concentration c was taken in the form:

$$\frac{\partial \bar{c}}{\partial t} + \frac{\partial(\bar{u}_i \cdot \bar{c})}{\partial x_i} = \frac{\partial}{\partial x_i} \left[\mu_c \frac{\partial \bar{c}}{\partial x_i} - (\bar{c} \bar{u}_i - \bar{c} \cdot \bar{u}_i) \right] + S_c,$$

where $i = 1, 2, 3$; t stands for the time, $x_i = (x, y, z)$ are the right-hand Cartesian coordinates, $\bar{u}_i = (\bar{u}, \bar{v}, \bar{w})$ are the resolved-scale components of the velocity vector, \bar{c} is the resolved-scale concentration of the tracer, S_c is the source term, and μ_c is the molecular diffusivity of the tracer. The overbar signifies the grid-cell volume average. The quantities $F_{si} = \bar{c} \bar{u}_i - \bar{c} \cdot \bar{u}_i$ are the components of the subgrid concentration flux, respectively, which were parameterized as $F_{si} = -K_c(\partial \bar{c} / \partial x_i)$. The value of subgrid turbulent diffusivity K_c was assumed to be equal to the subgrid thermal diffusivity. The latter quantity was parameterized through the product of subgrid length scale and square root of the subgrid turbulence kinetic energy as described in Fedorovich et al (2001a). Zero-gradient boundary conditions are employed for \bar{c} at the walls of

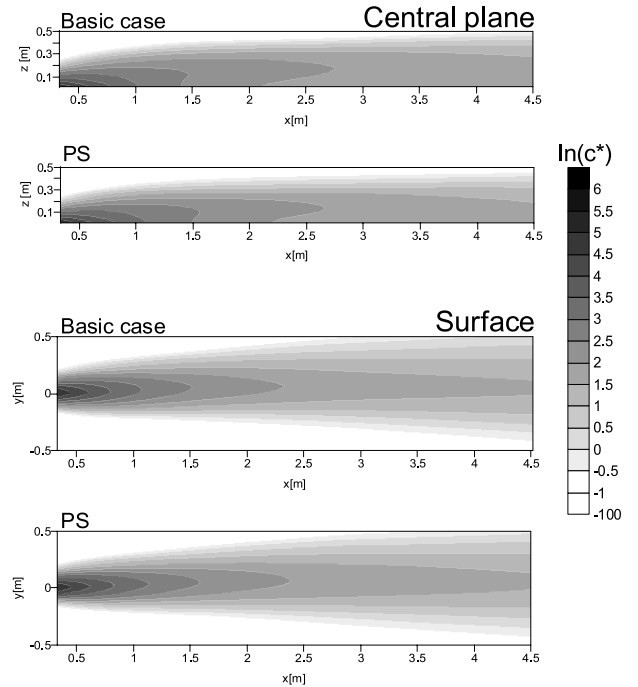


Fig. 5. Numerically simulated concentration distributions in the wind tunnel CBL with positive elevated wind shear (PS) and in the basic flow case (Basic case) without elevated shear. The source is at the ground level in both cases. The origin of the x -ordinate is at the source location. The capping-inversion and shear-zone elevations at $x=0$ are 300 mm

simulation domain (the wind-tunnel test section), and the radiation condition was applied at the outlet. In the grid cell containing the source, the source term had the form: $S_c = E_s / \Delta^3$, where E_s is the source strength and $\Delta^3 = \Delta x \Delta y \Delta z$ is the grid-cell volume. In all other grid cells of the simulation domain, the value of S_c was set equal to 0.

Numerically simulated concentration distributions for the basic CBL flow case with the shear-free inversion and for the CBL with imposed positive elevated shear are presented in Fig. 5. There is an overall agreement between the measured (Fig. 4) and computed (Fig. 5) concentration distributions with respect to their integral parameters. However, some important fine details of the tracer dispersion in the CBL such as plume-rise rate and surface concentration patchiness are rather poorly reproduced by the LES. The noted deficiencies are presumably due to insufficient spatial resolution of the conducted numerical simulations and spurious effects of the employed low-order advection scheme.

5. Plume dispersion in the non-steady CBL with shear

A comprehensive numerical study of passive tracer dispersion in the non-steady, horizontally (quasi-) homogeneous CBL has been reported by Dosio et al (2003). Following the Eulerian methodology, they added a conservation equation to the set of governing LES equations, previously employed for simulation of a variety of flow regimes in the atmospheric boundary layer. Similar methods to describe the tracer dispersion in the LES of CBL were previously used by Wyngaard and Brost (1984), Haren and Nieuwstadt (1989), Schumann (1989), and Henn and Sykes (1992). A different approach towards upgrading the LES for investigation of dispersion in the sheared CBL was exploited earlier by Mason (1992), who employed the Lagrangian framework to calculate the concentration patterns based on the LES-generated flow fields (see Sect. 6).

Wyngaard and Brost (1984) were first to demonstrate that properties of turbulent transport of the passive scalar emitted near the CBL bottom (bottom-up diffusion) are rather different from the transport of a scalar emitted at the inversion level (top-down diffusion). This

suggested bottom-up/top-down decomposition turned out to be very useful for the analyses of dispersion patterns in the shear-free CBLs. However, the concept and associated scaling still await extension for the case of sheared CBL with both surface- and elevated-shear contributions to the diffusive turbulent motions.

Dosio et al (2003) put numerical investigation of tracer dispersion in the CBL on a systematic basis and simulated dispersion regimes corresponding to four different values of geostrophic wind and three different values of surface heat flux in the simulation domain with a horizontal cross-section of $10\text{ km} \times 10\text{ km}$. The range of u_*/w_* in these numerical experiments was from 0.02 to 0.59. Thus, the CBL cases spanned in the study were from the practically shear-free CBL to the CBL with very significant contribution of surface shear to the turbulence production. Dispersion of plumes emitted from both the near-surface source ($z_s/z_i = 0.078$, where z_s is the source height) and the elevated source (placed almost in the middle of the CBL at $z_s/z_i = 0.48$) was studied.

Results of the aforementioned numerical experiments for the CBL cases with u_*/w_* in the range from 0.02 to 0.21 have shown very good agreement with experimental data available from the laboratory (water-tank) and field studies of dispersion from a near-surface source in the weakly sheared CBL, see left-hand panels in Fig. 6. Presented plots demonstrate the comparison of the computed vertical, σ_z and σ_z' , and horizontal (lateral), σ_y , dispersion parameters with experimental data. These dispersion parameters were evaluated in the following way:

$$\sigma_z^2 = \frac{\int c(z - \bar{z}) dV}{\int cdV}, \quad \sigma_z'^2 = \frac{\int c(z - z_s) dV}{\int cdV},$$

$$\sigma_y^2 = \frac{\int c(y - \bar{y}) dV}{\int cdV},$$

where \bar{z} and \bar{y} are the mean plume height and the mean plume horizontal position, respectively. The dimensionless distance from the source, X , in the plots is defined based on the Deardorff (1970b, 1985) convective scaling explained in Sect. 2 of the present paper.

At short distances from the source ($X < 1$), the simulation results for σ_z' were found to fit well with the expression $\sigma_z'/z_i = 0.52X^{6/5}$, which is

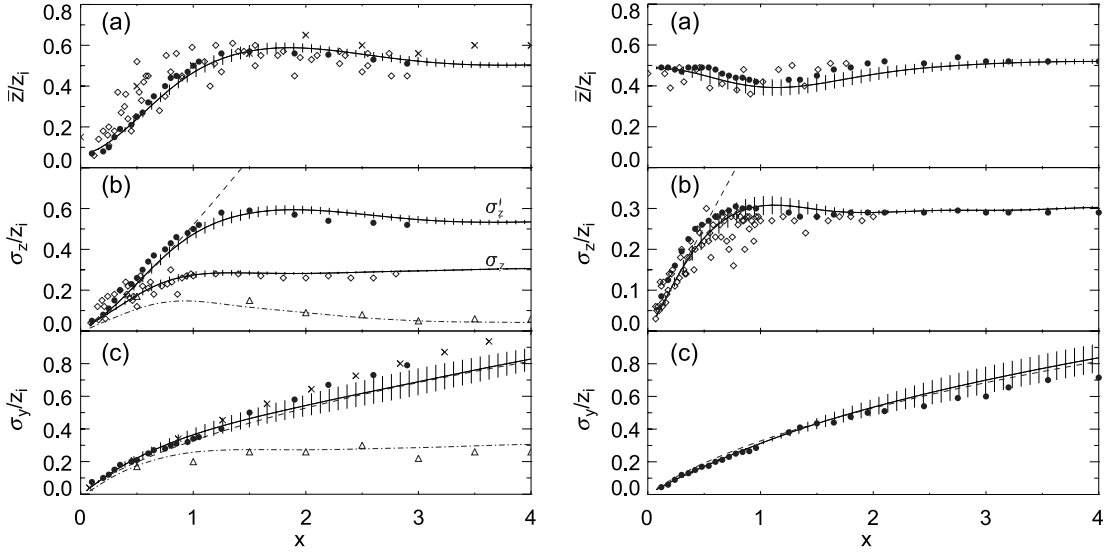


Fig. 6. Horizontal changes of the plume height and dispersion parameters σ_z , σ'_z , and σ_y in the almost shear-free CBL with near-surface (left-hand panels) and elevated (right-hand panels) sources; from Dosio et al (2003). The LES results from op. cit. are shown by solid lines with standard deviations indicated by vertical bars. Experimental data of Willis and Deardorff (1976), Weil et al (2002), and Briggs (1993) are shown by filled circles, \times symbols, and diamonds, respectively. The dashed lines represent $6/5$ and 1 power laws for σ'_z and σ_z (see explanations in the text), and the Gryning et al (1987) parameterization for σ_y . The dashed-dotted line illustrates the simulated meandering component as compared with the water-tank data of Weil et al (2002) shown by open triangles

very close to the classical approximation $\sigma'_z/z_i = 0.5X^{6/5}$ (Lamb, 1982). For the horizontal dispersion parameter σ_y , the LES results were in a good agreement with the laboratory data for $X < 2$. Besides that, they followed very closely the established analytical dependencies of σ_y/z_i on X discussed in the literature (Lamb, 1982; Briggs, 1985; Gryning et al, 1987).

Rather satisfactory agreement was also found between the LES results and experimental data for the plume emitted from the elevated source (right-hand panels in Fig. 6). For the vertical plume dispersion, only σ_z values are shown in the plots because the mean plume height in this case does not noticeably deviate from the initial release height and thus $\sigma'_z \approx \sigma_z$. The power-law dependence on X for σ_z/z_i retrieved from the LES confirmed the parameterization suggested by Lamb (1982) for dispersion from elevated releases at $X < 2/3$: $\sigma_z/z_i \simeq 0.5X$. The normalized lateral dispersion parameter σ_y/z_i as a function of X in the LES experiments with the elevated source followed approximately the same analytical curve as in the case of near-surface release, except for the region of small X , where the plume was spreading laterally slightly faster

in the case of the near-surface release due to the enhanced horizontal fluctuations at the surface. This was found consistent with the unified parameterization suggested by Lamb for both releases at $X > 1$: $\sigma_y/z_i \simeq (1/3)X^{2/3}$.

The LES results of Dosio et al (2003) are of special interest with respect to quantification of the surface-shear effect on the dispersion of a plume emitted at different elevations within the CBL. In order to account for the shear in the normalized concentrations patterns, the authors of op. cit. used a modified velocity scale w_m introduced through the empirical formula $w_m^3 = w_*^3 + 5u_*^3$ first suggested by Zeman and Tennekes (1977) for determination of velocity scale in the CBL with surface shear. The distance from the source x is then normalized as $X_m = (w_m/z_i)(x/U)$.

Numerical data presented in Fig. 7 (left-hand panels show results for the near-surface release and panels to the right refer to the elevated release) indicate that wind shear can considerably modify longitudinal variations of mean plume height and both vertical and lateral dispersion parameters in the CBL. As was mentioned in Sect. 3 of the present paper, the horizontal

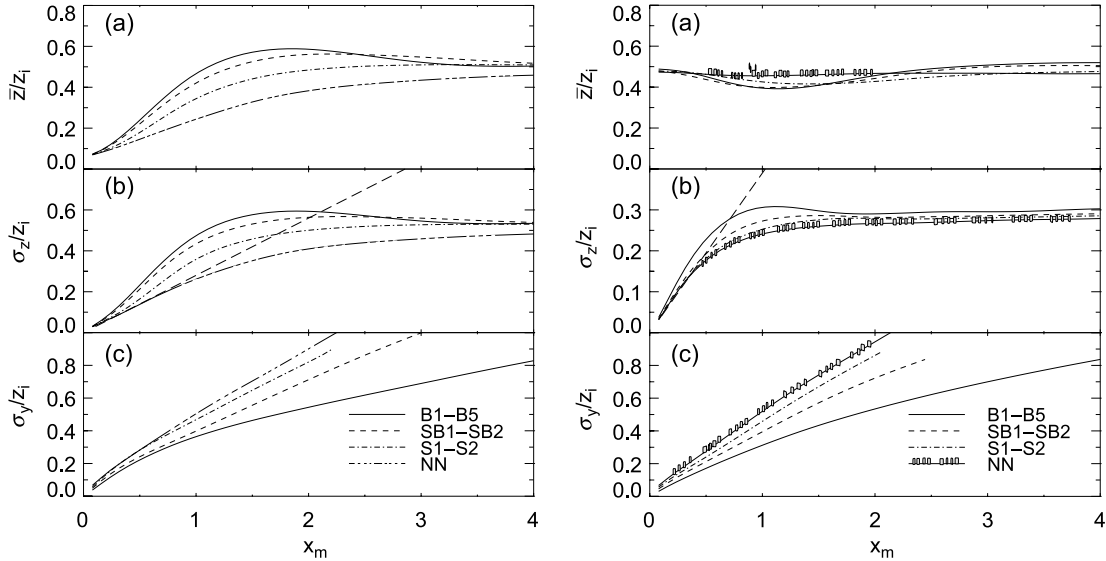


Fig. 7. Effects of surface wind shear on the plume height and dispersion parameters σ_z and σ_y in the CBL with near-surface (left-hand panels) and elevated (right-hand panels) sources; from Dosio et al (2003). The solid lines (cases B1–B5) show simulated parameters of the plume in the practically shear-free ($u_*/w_* \leq 0.21$) CBL. The dashed lines (SB1–SB2) correspond to the CBL cases with moderate shear ($u_*/w_* = 0.27$ and $u_*/w_* = 0.34$). The dashed and dotted lines refer to the strongly-sheared CBL cases ($u_*/w_* = 0.46$ and $u_*/w_* = 0.47$). The case of nearly-neutral boundary layer (indicated as NN) is represented by $u_*/w_* = 0.59$

velocity fluctuations throughout a significant portion of the CBL are considerably enhanced by surface wind shear. These turbulence regime changes, in addition to the faster longitudinal transport of tracer by larger mean velocities, lead to relatively less effective vertical dispersion in the sheared CBL and, consequently, to the slower plume rise with distance and smaller values of the vertical dispersion parameter σ_z . At the same time, the lateral spread of the tracer in the sheared CBL is intensified by enhanced horizontal velocity fluctuations, and the horizontal dispersion parameter grows with distance faster than in the case of shear-free CBL. The discussed shear effects on the tracer plume released at the surface are perfectly illustrated by the LES results shown in the left-hand panels of Fig. 7. Shear effects on dispersion in the CBL were generally less pronounced in the case of elevated release (right-hand panels in Fig. 7).

Employing Venkatram's (1988) idea of decomposition of lateral dispersion variance in “*b*” buoyancy- and “*s*” shear-related parts $\sigma_y^2 = \sigma_{yb}^2 + \sigma_{ys}^2$, and using the shear-contribution parameterization similar to the one that Luhar (2002) suggested for a coastal fumigation model, Dosio et al (2003) came up with a practicable expression

of σ_{ys}^2 for the case of near-surface release, (see eq. (32) in their paper), and a recommendation to use σ_{yb}^2 in the form proposed by Gryning et al (1987). Based on the LES data, rather feasible parameterizations were also developed for the vertical dispersion parameters σ_z and σ_z' . These parameterizations took into account surface-shear effects in the CBL cases with near-surface as well as with elevated plume releases, (see eqs. (35), (37), and (38) in Dosio et al, 2003).

Based on their LES results, Dosio et al (2003) concluded that the main effect of (surface) wind shear on the tracer dispersion in the atmospheric CBL is represented by a reduction of the vertical spread of a tracer, whereas its horizontal spread is enhanced. Consequently, the ground concentrations are strongly influenced as the increased wind tends to advect the plume for a longer time. The tracer, therefore, reaches the ground at greater distances from the source.

6. Lagrangian models of dispersion in the sheared CBL

According to the Lagrangian modeling methodology, the dispersion process is regarded as the change of the concentration when traveling

with a passive particle that moves with the turbulent flow (Nieuwstadt, 1998). The probability that a single particle released at time t_0 from position $\mathbf{r}_s \equiv (x_s, y_s, z_s)$, that is the source location, arrives at $\mathbf{r} \equiv (x, y, z)$ at time t is given by $p(\mathbf{r}, t; \mathbf{r}_s, t_0)$. Accordingly, the mean concentration c at (\mathbf{r}, t) is given by $c(\mathbf{r}, t) = \iiint p(\mathbf{r}, t; \mathbf{r}_s, t_0) c_0(\mathbf{r}_s) d\mathbf{r}_s$, where $c_0(\mathbf{r}_s)$ is the initial particle concentration distribution at \mathbf{r}_s . In the case of a point source with unit strength at \mathbf{r}_0 , the initial distribution is given by $c_0(\mathbf{r}_s) = \delta(\mathbf{r}_s - \mathbf{r}_0)$, where δ is the Dirac delta function. The integration provides $c(\mathbf{r}, t) = p(\mathbf{r}, t; \mathbf{r}_s, t_0)$, which means that in this case the mean concentration is equivalent to the single-particle probability density. The probability density function is calculated by releasing a large number of particles and, particle positions at each time being known, computing the number of particles within a given volume around \mathbf{r} . The particle position \mathbf{r}_p is found by integrating $d\mathbf{r}_p = \mathbf{u}_L dt$, where \mathbf{u}_L is the Lagrangian velocity of the particle.

The method to calculate the Lagrangian velocity is rather model-specific. Lagrangian models, employed in air pollution applications, use for this purpose the prescribed mean turbulent flow characteristics and parameterized turbulence statistics derived from measurement data or/and from some flow model output, see review by Wilson and Sawford (1996). When applied to calculation of concentration fields in the CBL, such Lagrangian models typically require specification of parameterizations for variances of the wind velocity components, components of the vertical turbulent shear stress, the turbulence kinetic energy (TKE) dissipation rate, the third moment of the vertical velocity fluctuations, and probability density distribution of these fluctuations. In the Lagrangian models, based on the LES-derived flow fields, the Lagrangian velocity is evaluated from the resolved velocity fields in combination with contribution from the subgrid velocity variances. The first model of this type was developed by Lamb (1978).

A representative example of applied Lagrangian model based on the parameterized description of CBL turbulence is the model of Rotach et al (1996), and de Haan and Rotach (1998). This random-walk type Lagrangian model is particularly designed to cover the whole flow regimes in the atmospheric boundary-layer flow with com-

bined surface-shear and buoyancy turbulence-generation mechanisms. In order to account for both these mechanisms, the probability density function (PDF) of the particle velocities is constructed as a weighted sum of a skewed (characteristic of the CBL flow) and a Gaussian PDF (representative of the velocity field in the neutral boundary layer), using the so-called transition function F_t . The function F_t is a continuous function of the inversion height z_i , hydrostatic stability expressed in terms of the Monin-Obukhov length scale L , and the current height z of each particle. It is specified in such a way that in fully convective conditions and sufficiently far away from underlying surface, F_t is set equal to unity, which corresponds to the situation, when the horizontal and vertical velocity fluctuations are not correlated. For neutral conditions and when approaching the surface, the distributions of u and w fluctuations are assumed to be jointly Gaussian, and $F_t = 0$. Due to limited data availability, the transition function has originally been calibrated from near-ground atmospheric measurements only. In a recent attempt by Kastner-Klein et al (2001) to improve the parameterization for F_t , as well as parameterizations for other turbulence characteristics employed in the model, the wind-tunnel data on the statistics of velocity fluctuations and on the TKE dissipation rate in the sheared CBL from Fedorovich et al (1996), Kaiser and Fedorovich (1998), and Fedorovich et al (2001) were additionally invoked.

The comparison of the original and new parameterizations for the velocity variances is presented in Fig. 8. It is clear from the first glance that only for the vertical velocity variance the original parameterization from Rotach et al (1996) works appropriately. For the horizontal velocity variances, the original parameterizations produce too large values of $\overline{u'^2}$ and $\overline{v'^2}$ in the main portion of the CBL and do not account for the fast decay of variances with height in the near-surface region of the flow.

Both original and modified turbulence parameterizations were incorporated in the Rotach et al (1996) Lagrangian model, and the model sensitivity to the turbulence parameterizations was studied for different locations downwind of the source. As reference data, the wind-tunnel concentration measurements and LES results described in Fedorovich and Thäter (2002), and Thäter et al (2001) were used. In Fig. 9, mean

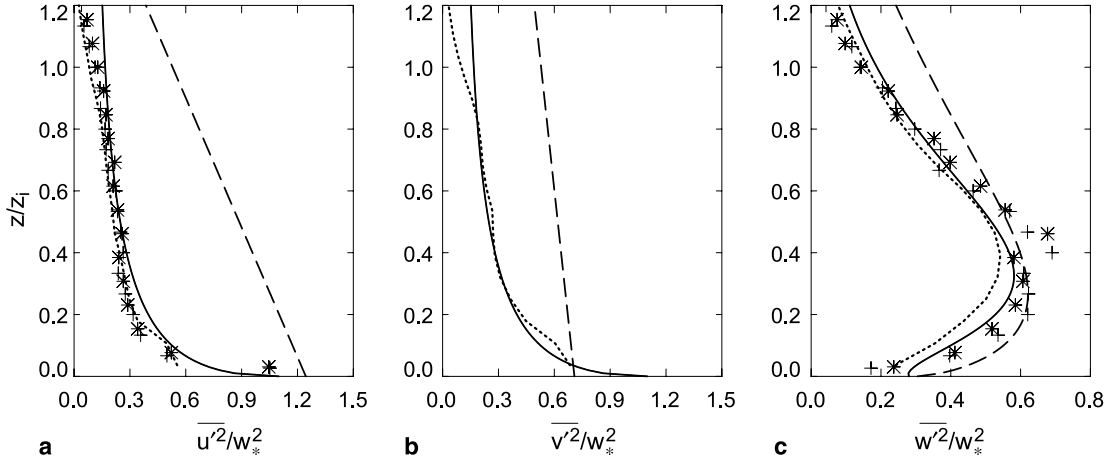


Fig. 8. Comparison of different Lagrangian-model parameterizations for velocity component variances with wind-tunnel and LES data of Fedorovich et al (1996; 2001a) for the sheared CBL. Asterisks and crosses present, respectively, wind-tunnel measurements at 2.3 m and 4.0 m downwind of the source location. The LES data at 2.3 m downwind of the source are given by dotted lines. Dashed lines show original parameterizations of the Rotach et al (1996) Lagrangian model. Solid lines present the modified parameterizations

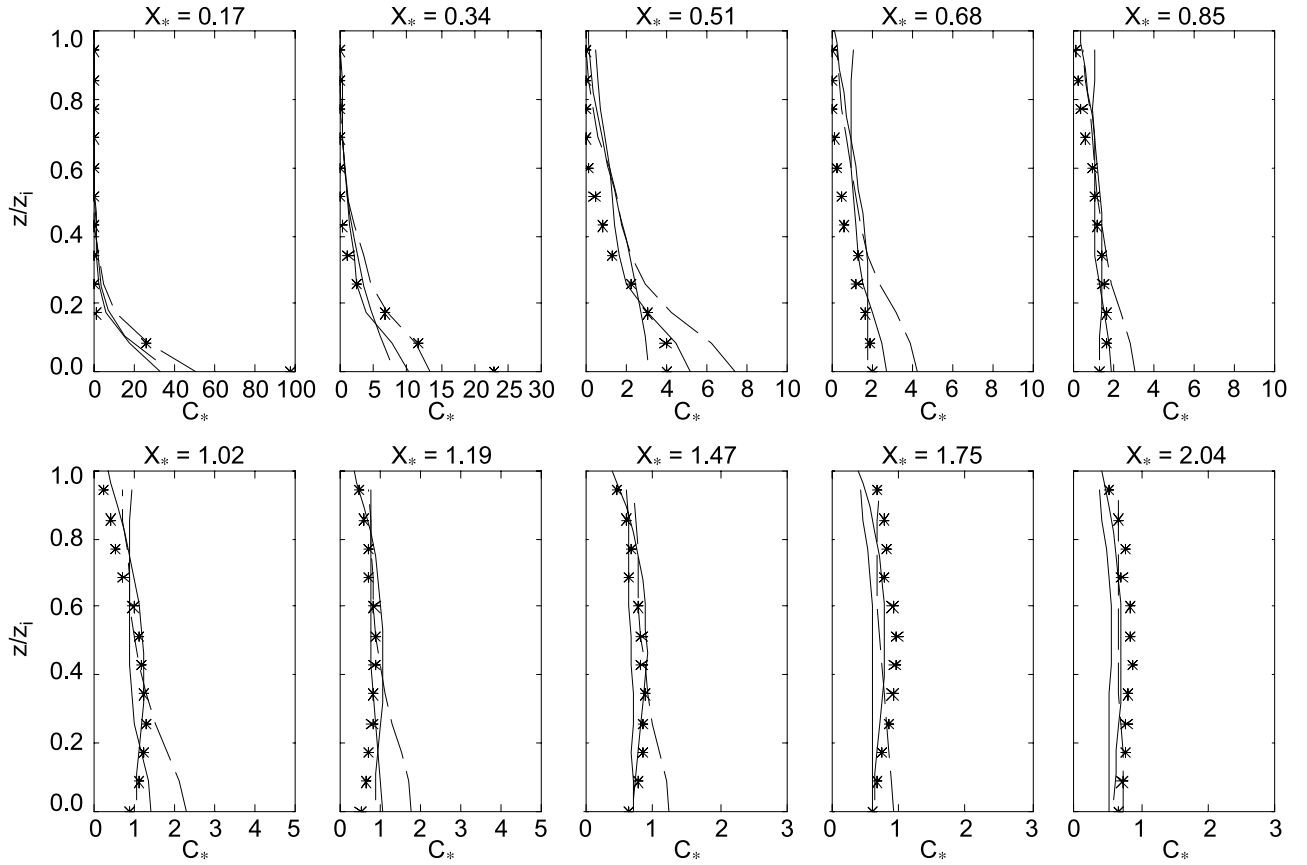


Fig. 9. Dimensionless mean concentration profiles along the plume centerline at different dimensionless distances x_* downwind of the ground-level source. The nondimensionalization is carried out with Deardorff (1985) convective scales. The Rotach et al (1996) Lagrangian model predictions with original turbulence parameterizations and with new turbulence parameterizations are presented by dashed and solid lines, respectively. The wind-tunnel measurements and LES calculations are shown by markers and by short-dashed lines, respectively

concentration profiles from the Lagrangian model runs with original and new turbulence parameterizations are shown at ten locations along the sheared CBL in comparison with wind-tunnel and LES profiles for the case of the ground-level source. The comparison clearly indicates that with modified turbulence parameterizations implemented, the Lagrangian model of Rotach et al (1996) is generally capable of successfully predicting dispersion from a ground source in the atmospheric CBL with moderate surface wind shear. Only at the first two locations does the model version with original parameterizations seem to perform better than the version with new parameterizations. At larger distances from the source, the model with original parameterizations considerably overestimates concentration values in the lower portion of the CBL. Both model versions fail to reproduce the maximum in the concentration profile that develops at $x_* \geq 1.02$. A similar maximum within this range of distances can be identified in the concentration profiles from LES. However, the vertical dispersion of tracer in LES at small distances from the source appears to be too large in comparison with the wind-tunnel data. This is apparently another deficiency of the employed LES based on the Eulerian approach, (see also discussion in Sect. 4).

The main advantage of the Lagrangian LES-based dispersion modeling approach is its capability to ensure, numerically, in an easier and more predictable manner, the conservation of mass of the tracer and its positive definiteness, and to minimize the spurious effects of numerical diffusion and dispersion (Nieuwstadt, 1998). This feature of the Lagrangian approach makes it especially useful for LES of dispersion in the sheared CBL characterized by fast advection of the tracer. Under such conditions, LES based on the Eulerian methodology usually requires special nonlinear numerical schemes, which make its less computationally efficient.

Recently, a LES-based Lagrangian model study of dispersion in CBLs with varying degrees of wind shear was reported by Weil et al (2001). For simulating the CBL turbulent flow, they employed the LES code of Moeng and Sullivan (1994) with the subgrid turbulence closure described in Sullivan et al (1994). The Lagrangian velocities of the particles were

calculated from the sum of resolved velocities and random subgrid-scale velocities using a detailed stochastic model of Thomson (1987). The LES runs were conducted for $-z_i/L = 5.5$ (strongly sheared CBL), 16, and 106 (almost shear-free CBL). Only the case of ground-level source was investigated.

It was found that the curves of the normalized mean plume (subscript p) height z_p/z_i versus dimensionless downstream distance $X = xw_*/(Uz_i)$ for different $-z_i/L$ collapse to essentially the same one for $X < 0.1$ (with $z_p/z_i \propto X$), but exhibit a natural ordering by stability for larger distances. The normalized plume height for the case of weak shear was the largest followed by those for moderately and strongly sheared CBLs. This result is consistent with the LES data of Dosio et al (2003) obtained using the Eulerian method for the simulation of the tracer dispersion (see Fig. 7). In the simulated CBL case with strong shear ($-z_i/L = 5.5$), the normalized plume height z_p/z_i was following $X^{2/3}$ dependence over the range of distances $0.25 < X < 0.9$. This was found close to the well-known behavior of surface release in the neutral boundary layer.

The dependence of the surface crosswind-integrated concentration, C^y , on X showed a general consistency with the plume-height variation. For weak shear ($-z_i/L = 106$), the decrease of C^y with X ($\propto X^{-2}$) was greater than expected in the absence of along-wind diffusion ($\propto X^{-5/4}$), which allowed Weil et al (2001) to conclude that this diffusion was important in the simulated weak-shear case. With strong shear ($-z_i/L = 5.5$), C^y varied as $X^{-2/3}$ within the same range of X , where the dependence of z_p/z_i on X was close to the neutral-layer behavior.

Weil et al (2001) compared their simulated crosswind-integrated concentrations with field data from the Prairie Grass and CONDORS (Briggs, 1993) experiments and found that simulated C^y followed the average data trend for different $-z_i/L$ rather well, although there was a considerable scatter in the field data for $X > 0.3$.

7. Concluding remarks

The state-of-the-art laboratory and numerical model approaches towards the description of

dispersion processes in the atmospheric convective boundary layer with surface and elevated wind shears have been reviewed. In the review of numerical models, emphasis was laid on the Large Eddy Simulation (LES) of dispersion. Presently, LES is primarily used as a scientific tool. However, one may expect that with growing computer power, this simulation technique will be employed more frequently as an applied research tool in dispersion studies.

The reviewed results of laboratory and numerical studies have indicated that wind shears can have a significant impact on various characteristics of dispersion in the CBL. The plume height, ground-level concentration, vertical and horizontal dispersion parameters, and crosswind-integrated concentrations in the CBL are all affected to a certain extent by wind shears. The continued development of LES and the forthcoming implementation of Direct Numerical Simulation (DNS), which seems to be not very remote, in the studies of atmospheric dispersion on surface- and boundary-layer scales, will provide researchers with data on more detailed dispersion characteristics such as concentration fluxes, variances, and higher-order statistics.

The analyses and interpretations of these new numerical data will not be conclusive and complete without new laboratory and field experimental data available for verification of numerical simulations. As was mentioned in the Introduction, there were no major field experiments organized during the last decade specifically designed to study the tracer dispersion in the sheared CBL, and the author of this review has heard of no plans within the atmospheric dispersion community of putting together such an experiment in the near future. Laboratory studies of dispersion (both with water tanks and wind tunnels) are also losing ground all over the world due to their high costs and non-attractiveness to researchers of the younger generation, who tend to seek only numerical solutions to scientific problems. In this sense, the future of boundary-layer dispersion studies crucially depends on the readiness of the scientific community, and society in general, to invest money and effort in the adequate experimental facilities and programs.

Acknowledgements

The author gratefully acknowledge productive discussions with Petra Kastner-Klein, Johannes Thäter, and Robert Conzemius in the course of preparation of this review. Many thanks also to Natascha Kljun for the plots with the Lagrangian model data. The reviewed research was partially supported by the Deutsche Forschungsgemeinschaft (DFG) within the Project Ji 18/5 and National Science Foundation (USA) within the grant ATM-0124068.

References

- Briggs GA (1985) Analytical parameterization of diffusion: the convective boundary layer. *J Clim Appl Meteor* 24: 1167–1186
- Briggs GA (1993) Plume dispersion in the convective boundary layer. Part II: Analyses of CONDORS field experiment data. *J Appl Meteor* 32: 1388–1425
- Conzemius R, Fedorovich E (2002) Dynamics of convective entrainment in a heterogeneously stratified atmosphere with wind shear. Proc. 15th AMS Symp. on Boundary Layers and Turbulence, 15–19 July 2002, Wageningen, The Netherlands, pp 31–34
- Conzemius R, Fedorovich E (2003) Evolution of mean wind and turbulence fields in a quasi-baroclinic convective boundary layer with strong wind shears. Proc. 11th Int. Conf. on Wind Eng., 2–5 June 2003, Lubbock, Texas, USA, pp 2055–2062
- Csanady GT (1978) Turbulent interface layers. *J Geophys Res* 83: 2329–2342
- Deardorff JW (1970a) Preliminary results from numerical integration of the unstable boundary layer. *J Atmos Sci* 27: 1209–1211
- Deardorff JW (1970b) Convective velocity and temperature scales for the unstable planetary boundary layer and for Raleigh convection. *J Atmos Sci* 27: 1211–1213
- Deardorff JW (1985) Laboratory experiments on diffusion: the use of convective mixed-layer scaling. *J Clim Appl Meteor* 24: 1143–1151
- Deardorff JW, Willis GE (1982) Ground-level concentrations due to fumigation into an entraining mixed layer. *Atmos Environ* 16: 1159–1170
- Deardorff JW, Willis GE (1984) Ground-level concentration fluctuations from a buoyant and non-buoyant source within a laboratory convectively mixed layer. *Atmos Environ* 18: 1297–1309
- Deardorff JW, Willis GE (1985) Further results from a laboratory model of the convective planetary boundary layer. *Bound Layer Meteor* 32: 205–236
- Deardorff JW, Willis GE, Stockton BH (1980) Laboratory studies of the entrainment zone of a convectively mixed layer. *J Fluid Mech* 100: 41–64
- Dosio A, Vilà-Guerau de Arellano J, Holtslag AAM, Builtjes PJH (2003) Dispersion of a passive tracer in buoyancy- and shear-driven boundary layer. *J Appl Meteor* 42: 1116–1130
- Fedorovich E (1995) Modeling the atmospheric convective boundary layer within a zero-order jump approach: an extended theoretical framework. *J Appl Meteor* 34: 1916–1928

- Fedorovich E, Kaiser R, Rau M, Plate E (1996) Wind-tunnel study of turbulent flow structure in the convective boundary layer capped by a temperature inversion. *J Atmos Sci* 53: 1273–1289
- Fedorovich E, Kaiser R (1998) Wind tunnel model study of turbulence regime in the atmospheric convective boundary layer. In: *Buoyant convection in geophysical flows* (Plate EJ et al, eds), Kluwer, pp 327–370
- Fedorovich EE, Mironov DV (1995) A model for shear-free convective boundary layer with parameterized capping inversion structure. *J Atmos Sci* 52: 83–95
- Fedorovich E, Nieuwstadt FTM, Kaiser R (2001a) Numerical and laboratory study of horizontally evolving convective boundary layer. Part I: Transition regimes and development of the mixed layer. *J Atmos Sci* 58: 70–86
- Fedorovich E, Nieuwstadt FTM, Kaiser R (2001b) Numerical and laboratory study of horizontally evolving convective boundary layer. Part II: Effects of elevated wind shear and surface roughness. *J Atmos Sci* 58: 546–560
- Fedorovich E, Thäter J (2001) Vertical transport of heat and momentum across a sheared density interface at the top of a horizontally evolving convective boundary layer. *J Turbulence* 2: 007
- Fedorovich E, Thäter J (2002) A wind tunnel study of gaseous tracer dispersion in the convective boundary layer capped by a temperature inversion. *Atmos Environ* 36: 2245–2255
- Garratt JR, Wyngaard JC, Francy RJ (1982) Winds in the atmospheric boundary layer: prediction and observation. *J Atmos Sci* 39: 1307–1316
- Gryning S-E, Holtslag AAM, Irwin JS, Siversten B (1987) Applied dispersion modeling based on meteorological scaling parameters. *Atmos Environ* 21: 79–89
- de Haan P, Rotach MW (1998) A novel approach to atmospheric dispersion modelling: the puff-particle model (PPF). *Q J Roy Meteor Soc* 124: 2771–2792
- Hanna SR, Paine RJ (1989) Hybrid plume dispersion model (HPDM) development and evaluation. *J Appl Meteor* 34: 206–224
- van Haren L, Nieuwstadt FTM (1989) The behavior of passive and buoyant plumes in a convective boundary layer, as simulated with a large-eddy model. *J Appl Meteor* 28: 818–832
- Henn DS, Sykes SR (1992) Large-eddy simulation of dispersion in the convective boundary layer. *Atmos Environ* 26A: 3145–3159
- Hibberd MF, Luhar AK (1996) A laboratory study and improved PDF model of fumigation into a growing convective boundary layer. *Atmos Environ* 30: 3633–3649
- Hibberd MF, Sawford BL (1994a) Design criteria for water tank models of dispersion in the planetary convective boundary layer. *Bound Layer Meteor* 67: 97–118
- Hibberd MF, Sawford BL (1994b) A saline laboratory model of the planetary convective boundary layer for diffusion studies. *Bound Layer Meteor* 67: 229–250
- Holtslag AAM, Duynkerke PG (eds) (1998) Clear and cloudy boundary layers. Royal Netherlands Academy of Arts and Sciences, Amsterdam, 372 pp
- Holtslag AAM, Nieuwstadt FTM (1986) Scaling the atmospheric boundary layer. *Bound Layer Meteor* 36: 201–209
- Hunt JCR (1998) Eddy dynamics and kinematics of convective turbulence. In: *Buoyant convection in geophysical flows* (Plate EJ et al, eds), Kluwer, pp 41–82
- Hunt JCR, Durbin PA (1999) Perturbed vortical layers and shear sheltering. *Fluid Dyn Res* 24: 375–404
- Jacobs RG, Durbin PA (1998) Shear sheltering and the continuous spectrum of the Orr-Sommerfeld equation. *Phys Fluids* 10: 2006–2011
- Kaiser R, Fedorovich E (1998) Turbulence spectra and dissipation rates in a wind tunnel model of the atmospheric convective boundary layer. *J Atmos Sci* 55: 580–594
- Kastner-Klein P, Fedorovich E, Kljun N, Rotach MW (2001) Dispersion of gaseous plume in the sheared convective boundary layer: evaluation of a Lagrangian particle model versus wind tunnel simulation data. Proc. 3rd Int. Symp. on Environmental Hydraulics, 5–8 December 2001, Tempe, Arizona, USA, 6 pp (ISEH 2001 Abstracts, 130)
- Khanna S, Brasseur JG (1998) Three-dimensional buoyancy- and shear-induced local structure of the atmospheric boundary layer. *J Atmos Sci* 55: 710–743
- Lamb RG (1978) A numerical simulation of dispersion from an elevated point source in the convective boundary layer. *Atmos Environ* 12: 1297–1304
- Lamb RG (1982) Diffusion in the convective boundary layer. In: *Atmospheric turbulence and air pollution modelling* (Nieuwstadt FTM, van Dop H, eds). Dordrecht: D. Reidel, pp 159–229
- Lenschow DH (1998) Observations of clear and cloud-capped convective boundary layers, and techniques for probing them. In: *Buoyant convection in geophysical flows* (Plate EJ et al, eds), Kluwer, pp 185–206
- Lesieur M, Métais O (1996) New trends in large-eddy simulations of turbulence. *Annu Rev Fluid Mech* 28: 45–82
- Luhar AK (2002) The influence of the vertical wind direction shear on dispersion in the convective boundary layer, and its incorporation in coastal fumigation models. *Bound Layer Meteor* 102: 1–38
- Mason PJ (1992) Large-eddy simulation of dispersion in convective boundary layers with wind shear. *Atmos Environ* 26A: 1561–1571
- Mason PJ (1994) Large-eddy simulation: A critical review of the technique. *Q J Roy Meteor Soc* 120: 1–26
- Meroney RN (1998) Wind tunnel simulation of convective boundary layer phenomena: simulation criteria and operating ranges of laboratory facilities. In: *Buoyant convection in geophysical flows* (Plate EJ et al, eds), Kluwer, pp 313–326
- Meroney RN, Melbourne WH (1992) Operating ranges of meteorological wind tunnels for the simulation of convective boundary layer (CBL) phenomena. *Bound Layer Meteor* 61: 145–174
- Moeng C-H, Sullivan PP (1994) A comparison of shear- and buoyancy-driven planetary boundary layer flows. *J Atmos Sci* 51: 999–1022
- Nieuwstadt FTM (1998) Review of diffusion processes in the convective boundary layer. In: *Buoyant convection in geophysical flows* (Plate EJ et al, eds), Kluwer, pp 371–399
- Ohya Y, Hayashi K, Mitsue S, Managi K (1998) Wind tunnel study of convective boundary layer capped by a strong inversion. *J Wind Eng* 75: 25–30

- Ohya Y, Tatuno M, Nakamura Y, Ueda H (1996) A thermally stratified boundary layer tunnel for environmental flow studies. *Atmos Environ* 30: 2881–2887
- Park OH, Seo SJ, Lee SH (2001) Laboratory simulation of vertical plume dispersion within a convective boundary layer. *Bound Layer Meteor* 99: 159–169
- Poreh M, Cermak JE (1984) Wind tunnel simulation of diffusion in a convective boundary layer. *Bound Layer Meteor* 30: 431–455
- Pino D, Vilà-Guerau de Arellano J, Duynkerke P (2003) The contribution of shear to the evolution of a convective boundary layer. *J Atmos Sci* 60: 1913–1926
- Piomelli U, Chasnov JR (1996) Large-eddy simulations: theory and applications. In: *Turbulence and transition modelling* (Hallbäck M et al, eds), Kluwer, pp 269–336
- Poreh M, Cermak JE (1985) Study of neutrally buoyant plumes in a convective boundary layer with mean velocity and shear. Proc. 7th AMS Symp. on Turbulence and Diffusion, November 12–15, 1985, Boulder, CO, pp 119–121
- Poreh M, Rau M, Plate E (1991) Design considerations for wind tunnel simulations of diffusion within the convective boundary layer. *Atmos Environ* 25A: 1250–1257
- Rau M, Bächlin W, Plate E (1991) Detailed design features of a new wind tunnel for studying the effects of thermal stratification. *Atmos Environ* 25A: 1258–1263
- Rau M, Plate E (1995) Wind tunnel modelling of convective boundary layers. In: *Wind climate in cities* (Cermak J et al, eds), Kluwer, pp 431–456
- Rotach MW, Gryning S-E, Tassone C (1996) A two-dimensional Lagrangian stochastic model for daytime conditions. *Q J Roy Meteor Soc* 122: 367–389
- Sada K (1996) Wind tunnel experiment on convective planetary boundary layer. *J Japan Soc Mech Eng* 58: 3677–3684
- Schumann U (1989) Large-eddy simulation of turbulent diffusion with chemical reactions in the convective boundary layer. *Atmos Environ* 23: 1713–1727
- Snyder WH, Lawson RE Jr, Shipman MS, Lu J (2002) Fluid modeling of atmospheric dispersion in the convective boundary layer. *Bound Layer Meteor* 102: 335–366
- Stull RB (1988) An introduction to boundary layer meteorology. Kluwer Academic Publishers, 666 pp
- Sullivan PP, McWilliams JC, Moeng C-H (1994) A subgrid-scale model for large-eddy simulation of planetary boundary-layer flows. *Bound Layer Meteor* 71: 247–276
- Sykes RI, Henn DS (1989) Large-eddy simulation of turbulent sheared convection. *J Atmos Sci* 46: 1106–1118
- Thäter J, Fedorovich E, Jirka G (2001) A combined numerical and laboratory study of dispersion from a point source in the atmospheric convective boundary layer with wind shear. Proc. 3rd Int. Symp. on Environmental Hydraulics (ISEH 2001), 5–8 December 2001, Tempe, Arizona, USA, 6 pp (ISEH 2001 Abstracts, 133–134)
- Thomson DJ (1987) Criteria for the selection of stochastic models of particle trajectories in turbulent flows. *J Fluid Mech* 180: 529–556
- Venkatram A (1988) Dispersion in the stable boundary layer. In: *Lectures on air pollution modeling* (Venkatram A, Wyngaard JC, eds), Am Meteor Soc, pp 228–265
- Weil JC, Snyder WH, Lawson RE Jr, Shipman MS (2002) Experiments on buoyant plume dispersion in a laboratory convection tank. *Bound Layer Meteor* 102: 367–414
- Weil JC, Sullivan PP, Moeng C-H (2001) Lagrangian modeling of dispersion in convective boundary layers with varying degrees of wind shear. Proc. 3rd Int. Symp. on Environmental Hydraulics (ISEH 2001), 5–8 December 2001, Tempe, Arizona, USA, 6 pp
- Willis GE, Deardorff JW (1976a) A laboratory model of diffusion into the convective boundary layer. *Q J R Meteor Soc* 102: 727–745
- Willis GE, Deardorff JW (1976b) On the use of Taylor's translation hypothesis for diffusion in the mixed layer. *Q J Roy Meteor Soc* 102: 817–822
- Willis GE, Deardorff JW (1978) A laboratory study of dispersion from an elevated source within a modeled convective planetary boundary layer. *Atmos Environ* 12: 1305–1311
- Willis GE, Deardorff JW (1981) A laboratory study of dispersion from a source in the middle of the convectively mixed layer. *Atmos Environ* 15: 109–117
- Willis GE, Deardorff JW (1983) On plume rise within a convective boundary layer. *Atmos Environ* 17: 2435–2447
- Willis GE, Deardorff JW (1987) Buoyant plume dispersion and inversion entrapment in and above a laboratory mixed layer. *Atmos Environ* 21: 1725–1735
- Wilson JD, Sawford BL (1996) Review of Lagrangian stochastic models for trajectories in the turbulent atmosphere. *Bound Layer Meteor* 78: 191–210
- Wyngaard JC, Brost RA (1984) Top-down and bottom-up diffusion of a scalar in the convective boundary layer. *J Atmos Sci* 41: 102–112
- Zilitinkevich SS (1991) Turbulent penetrative convection. Avebury Technical, Aldershot, 179 pp
- Zeman O, Tennekes H (1977) Parameterization of the turbulent energy budget at the top of the daytime atmospheric boundary layer. *J Atmos Sci* 34: 111–123

Author's address: E. Fedorovich, School of Meteorology, University of Oklahoma, 100 East Boyd, Norman, USA (E-mail: fedorovich@ou.edu)